PAPER 57 (SESSION V)

Behaviour of lowcycle fatigue at elevated temperatures

T. KUNIO*, K. IWAMOTO†, K. KANAZAWA‡
*Professor, Dept. of Engineering, Keio University,
Koganei-shi, Tokyo, Japan.
†Head of Research Division, National Research Institute for Metals,
Meguro-ku, Tokyo, Japan.
‡Graduate student, Graduate School of Keio University, Japan.

Summary
The behaviour of fatigue cracks has been observed in order to clarify the process of low-cycle fatigue fracture. However, a large number of cracks, are initiated on a smooth specimen, a concept of 'crack density' is proposed to represent quantitatively the behaviour of fatigue cracks.

Fatigue tests on stainless steel push-pull specimens showed that under the same plastic strain range, an identical state of cracks is obtained in spite of the different conditions of temperature, provided that the cycle ratio is constant.

It is concluded that the process of low cycle fatigue fracture is influenced primarily by the plastic strain range, and that the rate of fatigue process depends on temperature, strain rate, and plastic strain energy per cycle.

Introduction

Phenomena of low cycle fatigue at elevated temperature are important from both industrial and theoretical points of view [1]. In the study of low cycle fatigue, many investigators have dealt with experimental relations between the number of strain cycles to failure and the test conditions [2], but few have dealt with the behaviour of low cycle fatigue cracks [3].

Because a large number of cracks are initiated on the surface of a smooth specimen subjected to high strain fatigue it is difficult to represent quantitatively their behaviour.

In this paper a concept of 'crack density' is proposed through which the processes of fatigue fracture are discussed. In addition, the factors governing the rate of fatigue processes are specified by the relations between the number of strain cycles to failure and the test conditions. Finally, the propagation of a crack in a notched specimen is discussed.

Definition of 'crack density' and experimental procedure

Many cracks initiate and propagate on the surface of a smooth specimen, so that it is impossible to predict which crack will lead to fracture of the specimen. On a cylindrical surface of unit length the number of cracks existing in a strip of the width ds is expressed as n, see Fig. 1., n is

the number of cracks intersecting the meridian line at the distance s, as $ds \to 0$. The mean value of n at s i.e. $\bar{n}$ the crack density, is given by:

$$\bar{n} = \frac{1}{2\pi r} \int_0^{2\pi r} n ds \qquad (1)$$

where r is the radius of the cylindrical surface.

It should be noticed that $\bar{n}$ is not the number of cracks itself but a value which increases with the initiation of new cracks and propagation of existing cracks; the initiation and propagation of cracks are not distinguished in the concept of crack density. The following facts, however, have been clarified by preliminary microphotographic observations [4]. The value of $\bar{n}$ depends primarily on the number of cracks, and large cracks on the surface of the specimen propagate into the interior of the specimen, while small cracks on the surface of the specimen do not propagate deeply. Accordingly, it is possible to find the constitution of cracks existing on the specimen by investigating the distribution of $\bar{n}$ from the surface to the interior of the specimen.

Fatigue tests were carried out in a push-pull testing machine on an austenitic stainless steel (AISI 321); its chemical composition is given in Table 1. The material was pre-heated for one hour at 600 °C heated for another hour at 1150 °C, and then water-quenched. After heat treatment, the specimen was machined and polished with No. 800 emery paper. Fig. 2 shows the specimen dimensions. The cracks were magnified 100 times for observation under a microscope.

Behaviour of fatigue cracks

Fig. 3 shows the relations between the plastic strain range and the number of strain cycles to failure N_f. For the test conditions indicated by the solid marks in Fig. 3, specimens were partially fatigued to a predetermined fraction of N_f, designated by N/N_f, where N is the number of repeated strain cycles, and were then removed from the testing machine. The surface of a specimen was electropolished uniformly in order to examine the interior of the specimen.

Fig. 4 shows the distribution of $\bar{n}$ from the surface to the interior of the specimen. It should be noted that the distribution of $\bar{n}$ depends primarily upon the plastic strain range. Under the condition of a large plastic strain, i.e. 1·2%, $\bar{n}$ on the original surface is large in the early stage of N/N_f, but decreases rapidly with increasing of depth. No cracks could be observed beyond a certain depth. These results imply that cracks initiate only at the surface. For a small plastic strain range, $\bar{n}$ at the surface is not so large as in the case of a large plastic strain range, but in the interior of the specimen, cracks are observed up to the same depth as in both cases.

To study the behaviour of fatigue cracks with endurance, the authors considered $\bar{n}$ at the outer surface and the depth below the surface at which $\bar{n}$ becomes 0·3/cm (designated by $d_{0\cdot3}$). The depth at which $\bar{n}$ becomes 0·3/cm is used as the depth of the deepest crack.

Fig. 5 shows the relation between $\bar{n}$ at the outer surface and N. In this figure, $\bar{n}$ at the original surface varies with the test conditions, even if the same number of strain cycles to failure are obtained under different test conditions. Fig. 6 shows the relations between $\bar{n}$ at the outer surface and N/N_f. It should be noted that under the same plastic strain range, the same value of crack density is obtained in spite of the different condition of temperature, provided that N/N_f is kept fixed. For a large plastic strain range, $\bar{n}$ at the outer surface is larger than that for the small plastic strain range at every stage. In the latter half of N_f, the increasing rate of $\bar{n}$ at the outer surface becomes smaller with N/N_f.

The depth $d_{0\cdot3}$ is plotted against N/N_f on Fig. 7. These depths increase rapidly in the latter half of N_f. There is no considerable difference in the test conditions, but for a small plastic strain range this depth becomes slightly larger than that for the large plastic strain range in the latter half of N_f.

The relationship between $\bar{n}$ at the outer surface and the depth $d_{0\cdot3}$ are given in Fig. 8. For the large plastic strain range (e.g. 1·2%), $\bar{n}$ at the outer surface becomes large in the first half of N_f, but the increase of $d_{0\cdot3}$ is not so large. In the latter half of N_f the depth increases rapidly, in spite of the small increase of $\bar{n}$ at the outer surface. The slope of the curve describing the relation between $\bar{n}$ and the depth $d_{0\cdot3}$ for the small plastic strain range is almost the same as that of the latter half of N_f for the large plastic strain range.

These results, show that the behaviour of fatigue cracks depends primarily upon the conditions of the plastic strain range. In the large plastic strain range, many cracks initiate on the surface of the specimen and the crack density $\bar{n}$ at the outer surface becomes large, in the early stage of the fatigue process. The size of cracks on the surface is small, and the depth is small, too. In the latter half of N_f, all cracks do not propagate in the same way, some propagate on the surface and, simultaneoulsy, into the interior of the specimen. On the other hand, for the small plastic strain range, only a few cracks initiate and the value of $\bar{n}$ at the surface does not become so large as the value for the large plastic strain range in the first half of N_f. Therefore the increase of $\bar{n}$ at the surface depends mainly opon the propagation of cracks on the surface and into the interior of the specimen.

There are two possible ways of cracks' development. One is the independent propagation of separate cracks, and the other is the connection of one crack with another. When n at the outer surface of the specimen is

large, cracks are apt to grow by connecting with others. When $\bar{n}$ remains small, a crack usually grows independently.

Factors which govern the rate of fatigue process

In order to interpret the phenomena of fatigue, the term 'fatigue damage' is often used [5]. The exact meaning of fatigue damage, however, has not been clarified; in the propagation of a single crack, the depth of the crack is regarded as fatigue damage [6].

In the previous section, the state of cracks was represented by the distribution of $\bar{n}$ from the outer surface to the interior of the specimen. Accordingly, the state of cracks may be regarded as fatigue damage.

The experimental result that for the same plastic strain range an identical state of cracks is always observed in spite of a different condition of temperature, provided that the cycle ratio N/N_f is kept fixed, implies that for the same plastic strain range (e.g. $\Delta\epsilon_p = \Delta\epsilon_{p_1}$), the state of cracks, designated by D, changes with repeated strain cycles N (Fig. 9). If the relation between D and N could be assumed to be $D = f(k_1 \cdot N)$ under a certain condition $C-a$ (e.g. temperature $T = T_1$, strain rate $\dot{\epsilon} = \dot{\epsilon}_1$, etc.), the relation between D and N can be written as $D = f(k_2 \cdot N)$ under another test condition $C-b$ (e.g. $T = T_2$, $\dot{\epsilon} = \dot{\epsilon}_2$, etc.). Here the change of D depends on the plastic strain range and k depends on other test conditions. For the same state of cracks (e.g. $D = D_1$), Fig. 9, the change in state of cracks per cycle is $dD/dN = k_1 \cdot f'(k_1 \cdot N_1)$ for the condition C $-$ a and $dD/dN = k_2 \cdot f'(k_2 \cdot N_2) = k_1 \cdot f'(k_1 \cdot N_1)$ for the condition C $-$ b, where N_1 and N_2 are the number of strain cycles to the state of cracks $D = D_1$ under the conditions $C-a$ and $C-b$, respectively. The relationships indicate that the rate of change of the same state of cracks is proportional to k, thus k must be a factor governing the rate of fatigue damage.

To clarify which test conditions determine the character of k, the above relations were applied to the state of cracks at 'fracture'. The same state of cracks at fracture (i.e. $N/N_f = 1$) is obtained if the plastic strain range is kept the same, while different temperatures and frequencies of straining are imposed [7]. In Fig. 9, if the state of cracks at fracture is designated by D_0 for $\Delta\epsilon_p = \Delta\epsilon_{p_1}$, the relationships $D_0 = f(k_1 \cdot N_{f_1})$ and $D_0 = f(k_2 \cdot N_{f_2})$ where N_{f_1} and N_{f_2} are the number of strain cycles to failure under the conditions $C-a$ and $C-b$, respectively, are obtained. These relationships imply that $k \cdot N_f$ is a constant for the same plastic strain range. Thus the factors governing k can be determined if the dependence of N_f on the test conditions is known.

Fatigue tests were carried out under systematically selected test conditions; the relation between the plastic strain range and N_f is shown in Fig. 10. Under the same plastic strain range, it is clear that N_f depends on the temperature and frequency of straining, and on the plastic strain energy per cycle, U. The dependence of N_f on U is discussed in the Appendix, from which k is given by $k = C(T, \tau) \cdot U$, where T is temperature in °K, and τ is the reciprocal of the mean strain rate. To show the dependence of $C(T, \tau)$ on temperature, $U \cdot N_f$ is plotted against temperature for the same plastic strain range in Fig. 11; because $U \cdot N_f$ is independent of frequency at room temperature $C(T, \tau)$ is normalized by the value of the room temperature. The dependence of $C(T, \tau)$ on temperature and frequency of straining is shown in Fig. 12. For the same plastic strain range and frequency of straining, it is assumed that the strain rate is approximately constant in spite of the variation of temperature. From Fig. 12, the relation between $C(T, \tau)$ and T is given by:

$$C(T, \tau) = a \exp(-C_1/T) + b \tag{2}$$

Putting $C_1 = 7600$ and $b = 1$ gives close agreement with the experimental data. The value a depends on strain rate; its relation to τ is given by:

$$a = 2{\cdot}1 \times 10^3 \, \tau^{0{\cdot}37} \tag{3}$$

Accordingly, $C(T, \tau)$ is given by:

$$C(T, \tau) = 2{\cdot}1 \times 10^3 \, \tau^{0{\cdot}37} \exp(-7600/T) + 1 \tag{4}$$

Thus the factor k which governs the rate of fatigue damage is given by:

$$k = \{2{\cdot}1 \times 10^3 \, \tau^{0{\cdot}37} \exp(-7600/T) + 1\} U \tag{5}$$

The value of $k \cdot N_f$ which depends on the plastic strain range shown in Fig. 13, and is given by:

$$k \cdot N_f = 4{\cdot}2 \times 10^3/(\Delta\epsilon_p)^{0{\cdot}45} \tag{6}$$

The rate of crack propagation

If k is the factor governing the rate of propagation of the crack, it is predictable that the rate of crack propagation will be proportional to k for the same state of cracks.

To verify this, notched specimens (Fig. 2) were used to restrict the state of cracks and to allow the rate of crack propagation to be measured. Fig. 14 shows the relation between the plastic strain range and N_f. Two types of the fracture surface were observed as shown in Fig. 15. One is at the final broken region near the root of notch (A type) and the other is at the final broken region at the center of the specimen (B type). To indicate the position of the crack tip, the depth λ from the surface is introduced as shown in Fig. 15.

Striations were observed on the fracture surface under all test conditions and it is assumed that the striation spacing gives the rate of crack propagation at that point.

Fig. 16 shows the relation between λ and the striation spacing.

The rate of crack propagation at the same depth from the surface is indicated in Fig. 17 with the value of k obtained from equation 5. There are two groups according to the type of fracture surface, i.e., type A and type B. Each group is represented by a straight line of slope 1. They show that the rate of crack propagation at the same depth from the surface is proportional to k, thus, the value of $(d\lambda/dN)/k$ is a constant at a given λ, provided that the type of fracture is the same, (Fig. 18).

Conclusions

Push-pull fatigue tests were carried out on AISI 321 stainless steel, and the following conclusions obtained.

1. Behaviour of low cycle fatigue cracks which initiate and propagate on a smooth specimen, depends primarily on the condition of the plastic strain range.
2. When fatigue tests are carried out at the same plastic strain range under different conditions of temperature, an identical state of cracks is always observed, provided that the cycle ratio N/N_f is kept fixed.
3. For the same conditions of the plastic strain range, the state of cracks D changes with the number of repeated cycles N as given by $D = f(k \,.\, N)$, the factor k which governs the rate of fatigue damage, depends on temperature, strain rate, and plastic strain energy per cycle.
4. For the same state of cracks, the rate of crack propagation obtained is proportional to k.

Acknowledgments

The authors wish to express their gratitude to Mr T. Ueda, a Staff Member of the National Research Institute for Metals and Mr S. Iwanaga of the Toyota Central Research and Development Laboratories, INC., for their fruitful discussions. The authors are also indebted to the Staff of the Material Science Laboratory, Keio University for their assistance in conducting the experiments.

References

1. LANGER, B. F., 'Design of pressure vessels for low-cycle fatigue', *Trans. ASME, Ser. D*, vol. 84, No. 3, p. 565, 1962.
2. COFFIN, L. F., Jr., 'Cyclic strain and fatigue behaviour of metals in the creep range', *Proc. 1st Int. Conf. on Fracture*, p. 1543, 1965.
3. LAIRD, C. & SMITH, G. C., 'Crack propagation in high stress fatigue', *Phil. Mag.*, vol. 7, p. 847, 1962.
4. KANAZAWA, K., IWANAGA, S., KUNIO, T., IWAMOTO, K. & UEDA, T., *Trans. Japan Soc. Mech. Engr.*, vol. 34, No. 258, p. 243, 1968.
5. MARTIN, D. E., 'An energy criterion for low-cycle fatigue', *Trans, ASME, Ser. D*, vol. 83, No. 4, p. 565, 1961.

6. SIMIZU, M., HACHUNO, K., NAKAMURA, H. & KUNIO, T., *Trans. Japan Soc. Mech. Engr.*, vol. 30, No. 215, p. 780, 1964.
7. KANAZAWA, K., IWANAGA, S., KUNIO, Y., IWAMOTO, K. & UEDA, T., to be published.

Appendix

In order to clarify how mechanical test conditions influence low cycle fatigue fracture, fatigue tests were carried out using aged materials under the same conditions of temperature and frequency of straining. The materials were aged for 24 hours at 900 °C after the heat treatment described in the paper.

Fig. 19 shows the relation between the plastic strain range and N_f. For the same plastic strain range, N_f for the aged material is larger than N_f for the quenched material at both 490 °C and 700 °C. A reason for this is, that for the same plastic strain range the resulting stress range for an aged material is smaller than that for a quenched material (Fig. 20).

The plastic strain energy per cycle U which is related to the plastic strain range and the stress range, and indicated approximately by $\Delta\epsilon_p \,.\, \Delta\sigma$, is an important factor in determining fracture. Fig. 21 shows the relation between the plastic strain range and the product of U and N_f. There is no difference between the aged and quenched specimens at the same temperature.

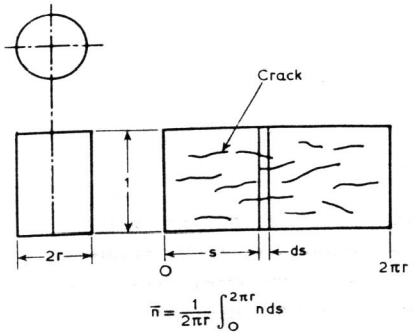

Fig. 1. Illustration of crack density.

Table 1. Chemical compositions %.

C	Si	Mn	P	S	Ni	Cr	Ti
0·04	0·58	1·72	0·027	0·006	10·90	18·01	0·39

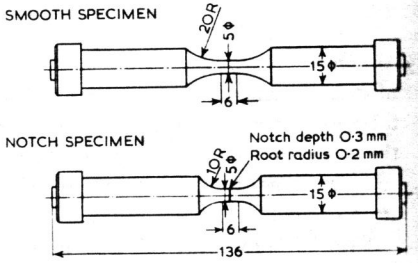

Fig. 2. Profiles of specimens (in mm).

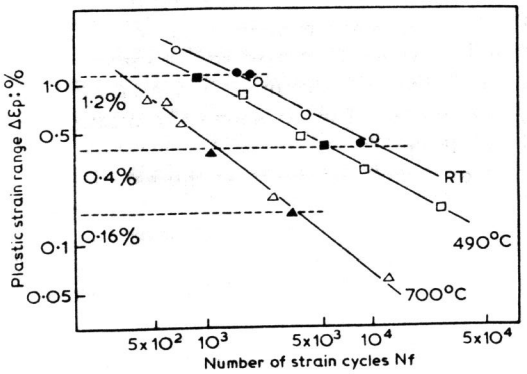

Fig. 3. Examples of the relation between the plastic strain range and the number of strain cycles to failure.

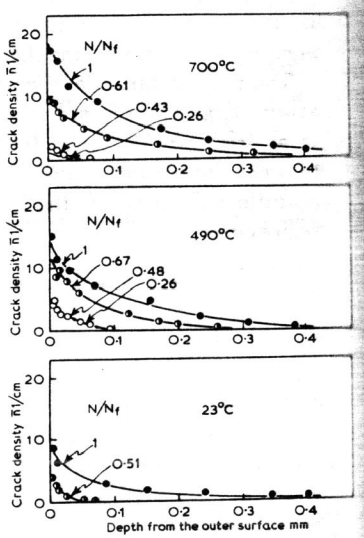

Fig. 4-2. Distributions of crack density from the surface to the interior of specimens at a plastic strain range of $\Delta\epsilon_p = 0{\cdot}4\%$.

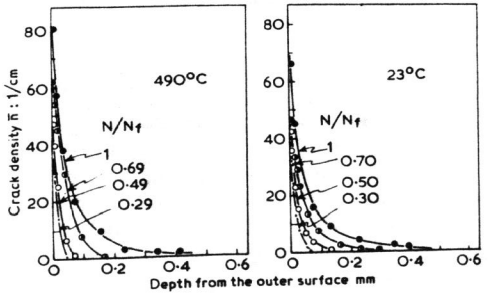

Fig. 4-1. Distributions of crack density from the surface to the interior of specimens at a plastic strain range of $\Delta\epsilon_p = 1{\cdot}2\%$.

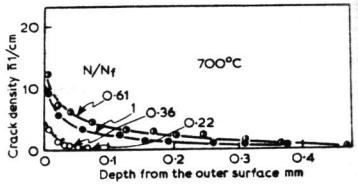

Fig. 4-3. Distributions of crack density from the surface to the interior of specimens at a plastic strain range of $\Delta\epsilon_p = 0{\cdot}16\%$.

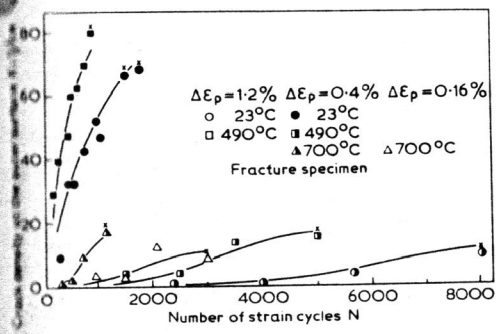

Fig. 5. Relation between crack density at the outer surface and repeated strain cycles.

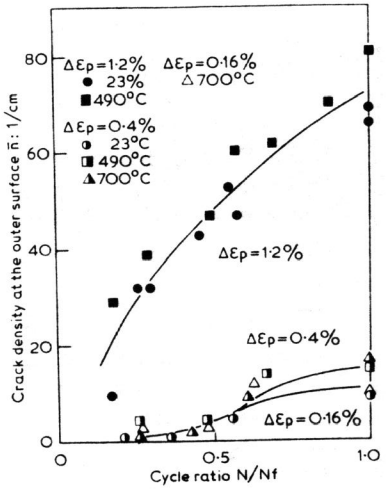

Fig. 6. Relation between crack density at the outer surface and the cycle ratio.

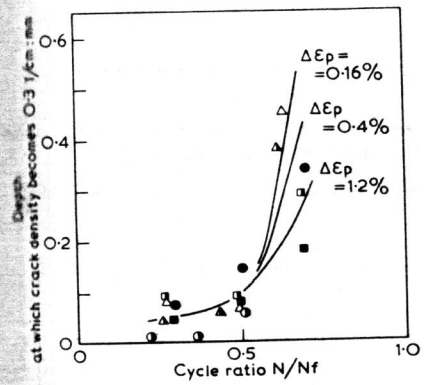

Fig. 7. Relation between the depth at which crack density becomes 0·3/cm and the cycle ratio (symbols indicate the same test conditions as in Fig. 5).

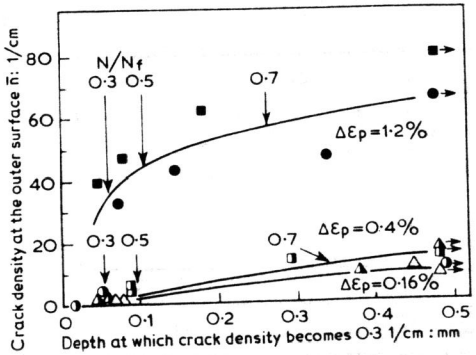

Fig. 8. Relation between crack density at the outer surface and the depth at which crack density becomes 0·3/cm (symbols indicate the same test conditions as in Fig. 5).

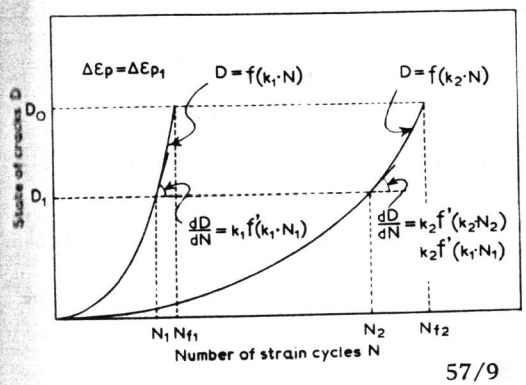

Fig. 9. Relation between the state of cracks and repeated strain cycles.

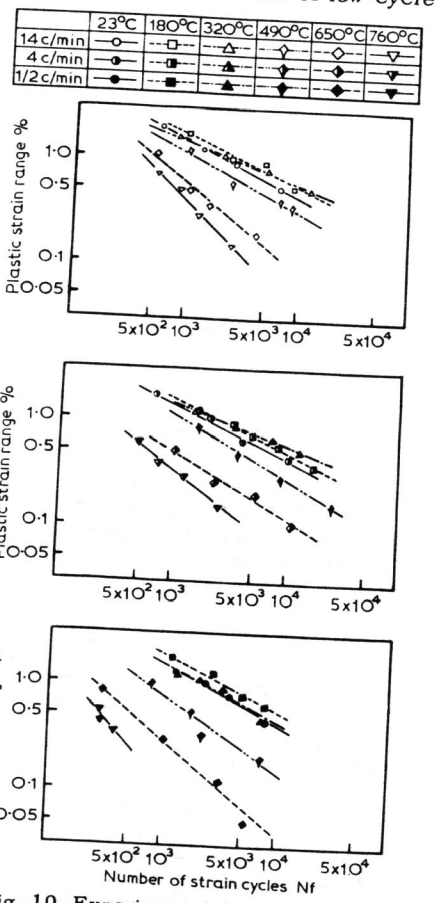

Fig. 10. Experimental data showing the relation between the plastic strain range and the number of strain cycles to failure (for smooth specimens).

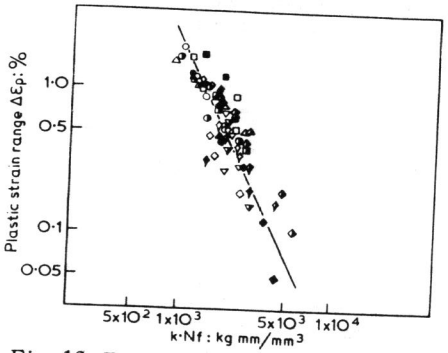

Fig. 13. Relation between the plastic strain range and k . Nf (symbols indicate the same test conditions as Fig. 10).

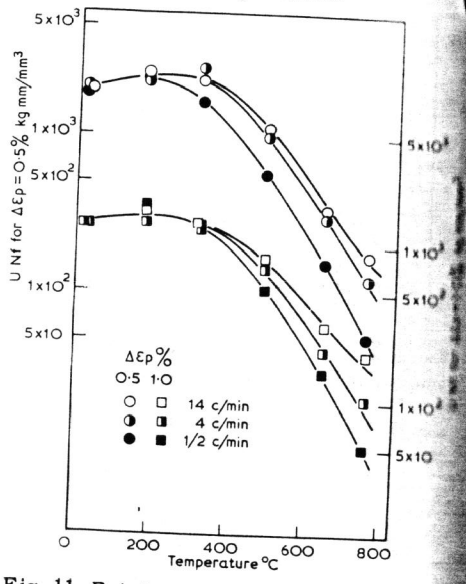

Fig. 11. Relation between U . Nf for the same plastic strain range and temperature.

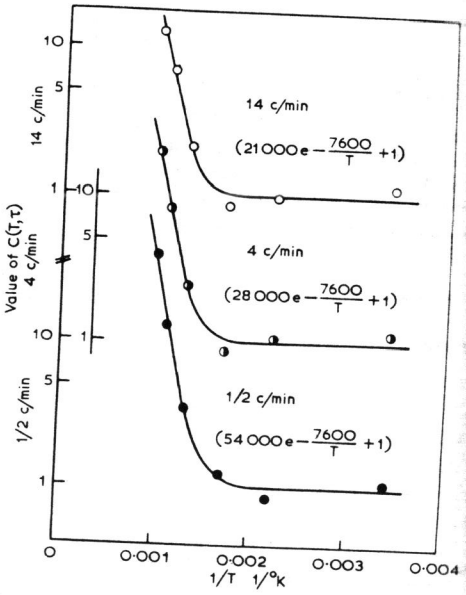

Fig. 12. Dependence of $C(T, \tau)$ on temperature at the plastic strain range of $\Delta\varepsilon_p = 0{\cdot}5\%$.

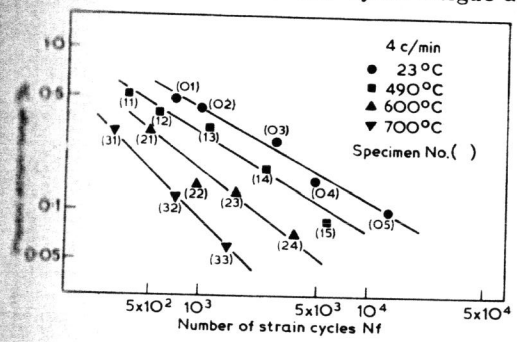

Fig. 14. Relation between the plastic strain range and the number of strain cycles to failure (for notch specimens).

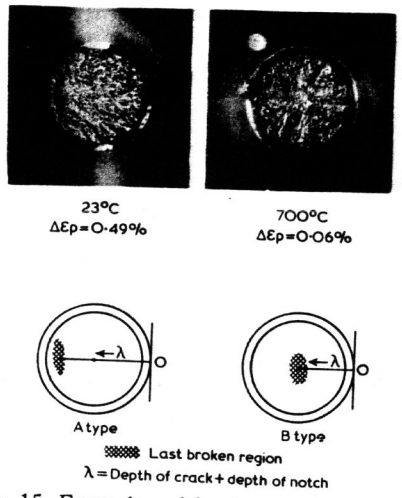

Fig. 15. Examples of fracture surface and definition of the site of crack tip.

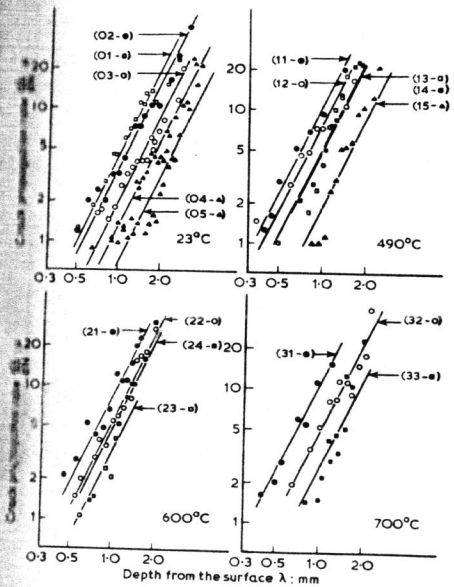

Fig. 16. Relation between λ and $\frac{d\lambda}{dN}$

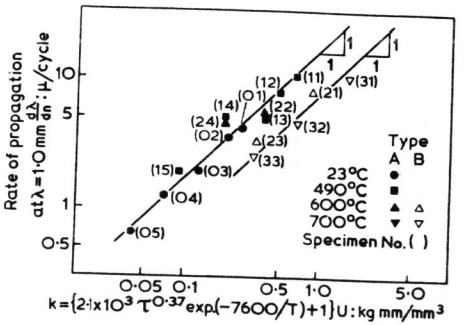

Fig. 17. Relation between $\overline{\frac{d\lambda}{dN}}$ and k at the depth of 1·0 mm from the surface.

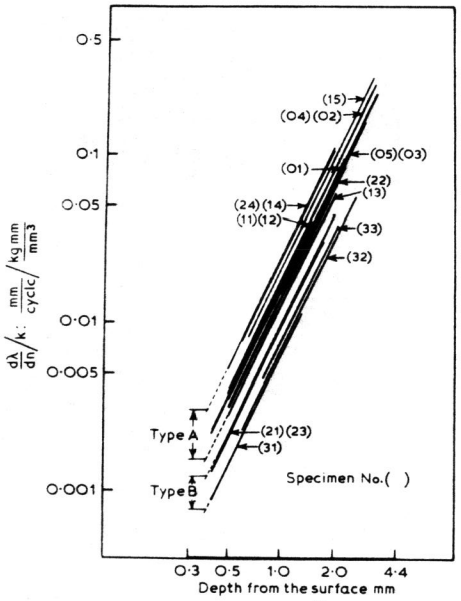

Fig. 18. Relation between $\frac{d\lambda}{dN}/k$ and λ.

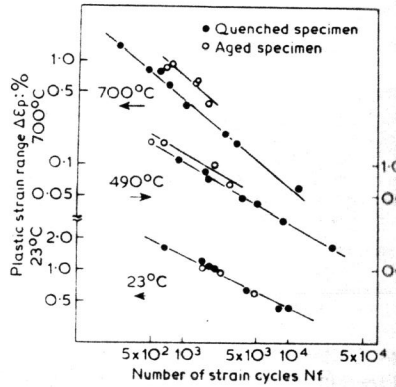

Fig. 19. Relation between the plastic strain range and the number of strain cycles to failure for the aged specimens and the quenched specimens.

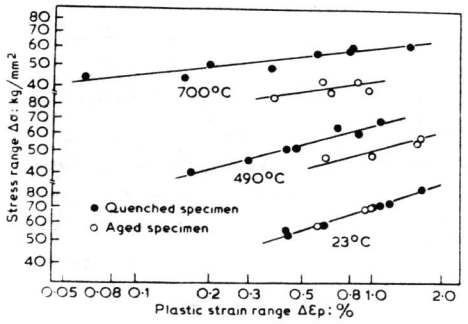

Fig. 20. Relation between the stress range and the plastic strain range for the aged specimens and the quenched specimens.

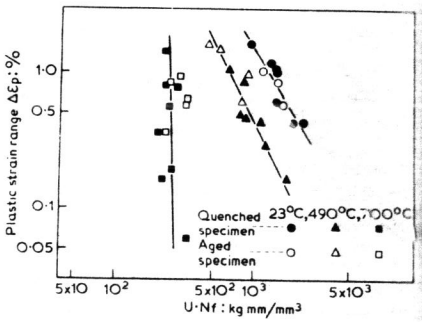

Fig. 21. Relation between the plastic strain range and the product of the plastic strain energy per cycle and the number of strain cycles to failure.